

Research Article pubs.acs.org/journal/ascecg

# **Neutral Hydrolysis of Post-Consumer Polyethylene Terephthalate** Waste in Different Phases

Patrícia Pereira, Phillip E. Savage,\* and Christian W. Pester\*



Cite This: ACS Sustainable Chem. Eng. 2023, 11, 7203-7209



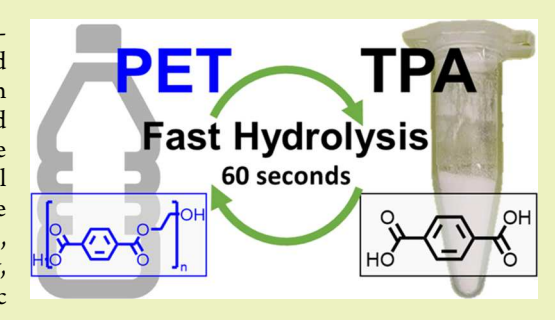
ACCESS I

Metrics & More

Article Recommendations

Supporting Information

ABSTRACT: Post-consumer polyethylene terephthalate (PET) was hydrolyzed in pure water over a wide range of temperatures (190-400 °C) and pressures (1-35 MPa) to produce terephthalic acid (TPA). Solid or molten PET was subjected to water as a saturated vapor, superheated vapor, saturated liquid, compressed liquid, and supercritical fluid. The highest TPA yields were observed for the hydrolysis of molten PET in saturated liquid water. Isothermal and non-isothermal hydrolysis of PET was also explored. Rapidly heating the reactor contents at about 5-10 °C/s ("fast" hydrolysis) led to high TPA yields, as did isothermal PET hydrolysis, but within 1 min instead of 30 min. Notably, these conditions resulted in the lowest environmental energy impact metric observed to date for uncatalyzed hydrolysis.



KEYWORDS: PET, fast hydrolysis, chemical recycling, environmental energy impact metric, saturated liquid

# **■ INTRODUCTION**

Over 80% of the 350 Mt of global plastic produced yearly ends as waste. Polyethylene terephthalate (PET) bottles, with a life cycle of less than 1 year, are ubiquitous in the waste. The United States recycles only 28% of its PET waste. Mechanical recycling is the predominant method for PET reuse. However, the involved material stresses reduce the chemical, thermal, and impact resistance of the resulting new material. As a result, the majority of recycled PET is downcycled (i.e., the final product has lower quality): PET bottles are mainly reprocessed into fiber for carpeting, which would then be landfilled or incinerated at the end of life.<sup>3,4</sup>

In contrast to mechanical approaches, chemical recycling aims to produce intermediate chemicals or monomers from the polymer waste. The resulting monomers can be repolymerized to a final product that is indistinguishable from the virgin polymer. Currently, solvolysis is the most studied path for chemical recycling of PET.5 One solvolysis technique, hydrolysis, decomposes PET into the monomers terephthalic acid (TPA) and ethylene glycol (EG). This approach is desirable considering that TPA is a dominant monomer in commercial PET production.<sup>6</sup> However, hydrolysis at neutral pH requires large amounts of water (up to a mass ratio of PET/water = 1:12), wastewater treatment, long reaction times at elevated temperatures (>250 °C), and high pressures (1-4 MPa).<sup>7–14</sup> While higher temperatures increase the rate of PET conversion, they also facilitate the undesirable decomposition of TPA. 15 Approaches to facilitate PET hydrolysis at lower temperatures include acid or base catalysis, 7,8,11,14 which, however, can still require long reaction times (up to 72 h) and add difficulties in handling corrosive reaction media. Mineral

acid-catalyzed hydrolysis additionally forms inorganic salt byproducts and generates wastewater with high concentrations of TPA. 16-18

This work centers on neutral hydrolysis to avoid the stated problems of acid and basic hydrolysis. Neutral hydrolysis of PET has been studied extensively. 19,20 Previous studies probed the influence of temperature and pressure on PET hydrolysis, showing that the TPA yield was higher in subcritical water than in supercritical water due to less product decomposition.<sup>8,13,21</sup> However, this prior work did not explicitly examine the dependence of TPA yields on the properties of the aqueous reaction medium.

This contribution elucidates the effects of conducting hydrolysis in different phases of water (saturated liquid, compressed liquid, saturated vapor, and supercritical) and determines the effects of temperature, pressure, and different post-consumer PET sources. While focus has conventionally been on isothermal hydrolysis, this work introduces "fast" hydrolysis as an alternative approach requiring just 1 min reactions. This approach was based on fast pyrolysis and fast hydrothermal liquefaction, which are rapid-heating processes that decompose organic material into energy-dense oils and gases within milliseconds to tens of seconds.<sup>22</sup> While fast

Received: February 16, 2023 Revised: April 14, 2023 Published: April 26, 2023





pyrolysis has been applied to waste plastics,<sup>23</sup> to the best of our knowledge, fast hydrolysis has not.

#### EXPERIMENTAL SECTION

PET Samples, Chemicals, and Reagents. Bottles that had held Perrier sparkling water (16.9 oz), Listerine mouthwash (500 mL), and Heinz ketchup (20 oz) served as representative post-consumer PET sources. Labels and caps were removed, and the bottles were cut into chips of roughly 6 × 8 mm (Table S1 and Figure S1). A Wiley Mill ground a representative sample of chips into 0.85 mm (20 mesh) particles. Products were recovered through dissolution in dimethyl sulfoxide (Millipore Sigma). Matrix-assisted laser desorption/ionization-time of flight mass spectrometry (MALDI-ToF-MS) used 2–5 dihydroxybenzoic acid (98%, Sigma-Aldrich) to obtain the oligomers' molecular weight. Control experiments used EG from Sigma-Aldrich and TPA from TCI. Deionized water was from an inhouse water purification system comprising ion exchange, reverse osmosis, high-capacity ion exchange, UV sterilization, and submicron filtration units.

Characterization of Post-Consumer PET. Thermogravimetric analysis (TGA) was performed by heating samples under  $N_2$  to 800 °C at 25 °C/min in an aluminum oxide crucible. Reconstructed air burned any char produced. Differential scanning calorimetry (DSC) was done under 20 mL/min  $N_2$ . Samples were heated from 20 to 300 °C, cooled to 50 °C, and again heated to 300 °C, all with a heating/cooling rate of 10 °C/min.

X-ray photoelectron spectroscopy (XPS) was performed on a Physical Electronics VersaProbe III with a monochromatic Al  $K_{\alpha}$  X-ray source ( $h\nu$  = 1486.6 eV) and a concentric hemispherical analyzer. Low-energy electrons (<5 eV) and argon ions were used for charge neutralization. The binding energy axis was calibrated using sputter-cleaned copper (Cu  $2p_{3/2}$  = 932.62 eV, Cu  $3p_{3/2}$  = 75.1 eV) and gold foils (Au  $4p_{7/2}$  = 83.96 eV). Peaks were referenced to the carbon C1s peak at 284.8 eV. The measurement takeoff angle was 45° to the sample surface plane. 95% of the signal originated from material within 3–6 nm of the surface. Quantification required instrumental relative sensitivity factors that accounted for the X-ray cross section and electrons' inelastic mean free path. The surface spot analyzed was ~200  $\mu$ m in diameter.

Procedure for PET Hydrolysis. Swagelok reactors comprised a stainless-steel port connector and two caps (nominal 1/2 in), resulting in 4 mL of internal volume. Some reactors had a thermocouple affixed to record interior temperatures throughout the reaction. The reactors were loaded with measured amounts of PET and deionized water and then sealed. Some reactors contained a metal wire insert that suspended the PET sample above the liquid phase (Figure S2) during the reaction.

An isothermal Techne fluidized sand bath at the desired set point temperature (e.g., the desired hydrolysis temperature for isothermal reactions between 200 and 400 °C) held the sealed reactors for the desired batch holding time (30 min and 2 h). The water loading and reactor temperature set the pressure within the reactor and determined whether the water was superheated vapor, saturated liquid, and vapor, compressed liquid, or in the supercritical state. For reactions in saturated liquid water, the amount of added water was calculated so that the liquid phase expanded to occupy 95% of the reactor volume at the sand bath set point temperature. Adding less water provided more headspace for saturated water vapor.

Removing the reactor from the sand bath (operating at 400–550 °C) after 1 min led to "fast" hydrolysis. The higher set point temperatures in the sand bath led to faster heating rates. The reactor never reached the set point temperature within the 1 min holding time (Figure S3).

Submerging heated reactors in room-temperature water immediately after they were removed from the sand bath quenched the reaction. Weighing the cooled reactors before and after opening provided the mass of gas phase products by difference. Pipetting aliquots of deionized water (10 mL total) into the reactor, withdrawing them and passing them through grade 1 cellulose filter

paper (from Whatman) in a reusable 25 mm filter holder (from Cole-Parmer) isolated the solids suspended in the water. Drying the filters, syringes, and reactors at 80 °C overnight permitted recovery of these suspended solids, which contained unconverted PET and the reaction product as a white solid. Drying the aqueous phase in a petri dish at 40 °C permitted recovery of any dissolved solids.

A minimum of three independent runs were performed under each experimental condition to provide mean values as best estimates for product yields and standard deviations as estimates of run-to-run variability.

Characterization of Hydrolysis Products. Adding 5 mL of dimethyl sulfoxide (DMSO) to the dried suspended solids dissolved TPA. The resulting solution of TPA in DMSO was passed through PTFE membrane filters (25 mm diameter) with a pore size of 1  $\mu$ m. The remaining solids contained unconverted PET and DMSO-insoluble byproducts. The yield, Y, of these undissolved solids (equation 1) is the ratio of their mass ( $m_{\rm undissolved\ solids}$ ) to the mass of PET loaded into the reactor ( $m_{\rm PET}$ ).

$$Y_{\text{undissolved solids}} \text{ (wt \%)} = \frac{m_{\text{undissolved solids}}}{m_{\text{PET}}} \times 100$$
 (1)

Matrix-assisted laser desorption/ionization-time of flight mass spectrometry (MALDI-ToF-MS, UltrafleXtreme Bruker) showed the molecular weights and identities of the repeat units and end groups of oligomers in the undissolved solids (see the Supporting Information). The instrument measured the signal from 0.5  $\mu$ L of dried droplets of a mixture of 5  $\mu$ L of 2,5-DHB (4 mg/mL) and 5  $\mu$ L of undissolved solids (4 mg/mL), both in phenol/chloroform, 2/3 (v/v). Conditions used were 500–5000 mass-to-charge ratio (m/z), two ion sources (25 and 22.16 kV), 9.10 kV lens with a reflector voltage of 26.44 kV, and an accelerator voltage of 13.48 kV, in positive ion mode.

A Shimadzu high-performance liquid chromatograph analyzed the DMSO solution using a Waters reversed-phase symmetry  $C_{18}$  column (5  $\mu$ m particle size, 150 mm × 4.6 mm) at 40 °C and an SPD-M20A photodiode array detector operating at 240 nm. The mobile phase was HPLC-grade acetonitrile at 0.1 mL/min and a 1 vol % H<sub>3</sub>PO<sub>4</sub> aqueous solution at 0.3 mL/min. The sample injection volume was 1  $\mu$ L. Analysis of standard solutions of the known TPA concentration in DMSO provided calibration curves. The TPA yield ( $Y_{\text{TPA}}$ , eq 2) is the ratio of the mass of TPA produced ( $m_{\text{TPA}}$ ) to the maximum TPA available, presuming the post-consumer material is entirely PET. The stoichiometry of the hydrolysis reaction is such that complete hydrolysis of a given mass of pure PET ( $m_{\text{PET}}$ ) would give 86% of that mass in TPA and the balance would be EG.

$$Y_{\text{TPA}} (\%) = \frac{m_{\text{TPA}}}{0.86 m_{\text{PET}}} \times 100$$
 (2)

Proton nuclear magnetic resonance spectroscopy ( $^{1}$ H NMR) was used to chemically characterize the dried suspended solids. A Bruker NMR DPX400 analyzed samples of about 6 mg of solids dissolved in 0.6 mL of deuterated DMSO at 400 MHz with a pulse length (90  $^{\circ}$ C) of 12.7  $\mu$ s, 2 s delay, 32 scans, and 4800 Hz spectral width.

A Shimadzu LCMS-8030 in negative ionization mode characterized the products in the aqueous phase with 3500–5000 V capillary voltage, 15 L/min  $N_2$  as the drying gas at 280 °C, and a 45 psi nebulizer. The mobile phase was 0.3 mL/min of 0.1% formic acid aqueous solution and 0.1 mL/min HPLC-grade acetonitrile. The injection volume was 1  $\mu$ L.

## ■ RESULTS AND DISCUSSION

Characterization of Post-Consumer PET. Table 1 provides results from the TGA and DSC of the different PET materials used in this study. The melting point for all three post-consumer PET samples was approximately 250 °C. Detailed TGA mass loss curves and experimental DSC curves can be found in the Supporting Information (Figure S4).

The enthalpy of melting,  $\Delta H_{\rm m}$  (J/g), and the cold crystallization enthalpy,  $\Delta H_{\rm cc}$  (J/g), were obtained through

Table 1. Results from Thermal Analysis of Chips Obtained from Post-Consumer PET Bottles

	moisture wt %	volatile matter wt %	fixed carbon wt %	ash wt %	$\begin{array}{c} \text{melting } T \\ (T_{\text{m,PET}}, {}^{\circ}\text{C}) \end{array}$
sparkling water bottle	0.20	85.6	9.4	4.8	250.4
ketchup bottle	0.00	87.8	12.2	0.0	247.6
Listerine bottle	0.00	91.2	7.7	1.1	249.9

the integration of DSC peaks (see Table 2). The crystallinity  $(X_c)$  of the PET samples was obtained by<sup>24</sup>

$$X_{\rm c} (\%) = \frac{\Delta H_{\rm m} - \Delta H_{\rm cc}}{\Delta H_{\rm m}^0} \times 100 \tag{3}$$

Table 2. Enthalpy of Melting  $(\Delta H_{\rm m})$ , Cold Crystallization Enthalpy  $(\Delta H_{\rm cc})$ , and Crystallinity  $(X_{\rm c})$  of PET Bottles Used in the Study

	sparkling water		Listerine		ketchup	
bottle type	bottom	body	bottom	body	bottom	body
$\Delta H_{\rm m}  (J/g)$	37.6	53.3	37.8	40.0	47.2	44.0
$\Delta H_{\rm cc}  ({\rm J/g})$	0	0	8.1	7.2	22.1	8.8
$X_{\rm c}$ (%)	27	38	21	23	18	25

 $\Delta H_{\rm m}^0$  is the melting enthalpy of 100% crystalline PET (140.1 J/g). <sup>24</sup> Table 2 shows that the crystallinity in the bottom of the PET bottles was consistently lower than that in the material body—an expected result considering the bottle's manufacturing via injection and blow molding. Most likely due to their different sizes, shapes, and processing conditions, the different post-consumer bottles studied herein had different overall degrees of crystallinity.

XPS was used to characterize the elemental composition of particles ground from PET bottle chips. The measured carbon (BE<sub>C1s</sub> = 284.8 eV) content (in atom %) was 74.4%, in good agreement with a theoretical value of 71.4% carbon for pure PET (see Figure SS). The experimental distribution of oxygen atoms (51% O–C and 48% O=C, Table S2) was in good agreement with the expected 50:50 distribution in the PET repeat unit. Similarly, the high-resolution C 1s carbon environment indicated the presence of  $\sim$ 7% of carbon atoms bound to heteroatoms in moieties such as alcohols, ethers, and amines. Some of these bonds (e.g., C–N) are hypothesized to result from additives (e.g., the green dye in the Perrier bottles).

Validation of Methods for TPA Recovery and Quantification. Reactors were loaded with TPA, EG, and water and held at either room temperature or at  $T=200~^{\circ}\mathrm{C}$  and t=2 h. Applying the product recovery and analysis protocol outlined above recovered 94.8  $\pm$  0.1% of the TPA in the control experiments at room temperature and 95.7  $\pm$  0.4% in the runs at 200  $^{\circ}\mathrm{C}$ . The aqueous phase contained 2% or less of the initial TPA. These control experiments show that the methods employed herein can recover and quantify about 95% of the TPA product within a mini-batch reactor.

Hydrolysis of Solid and Molten PET in Different Phases of Water. PET Hydrolysis at a Constant Temperature. PET hydrolysis was performed at  $T = 200 \,^{\circ}\text{C}$  for  $t = 2 \, \text{h}$  at different water loadings in the reactors. This provided the opportunity to assess the impact of saturated vs compressed

liquid water on the reaction while maintaining temperatures below the melting point of PET. Figure 1 shows the  $Y_{\text{TPA}} < 8\%$ ,

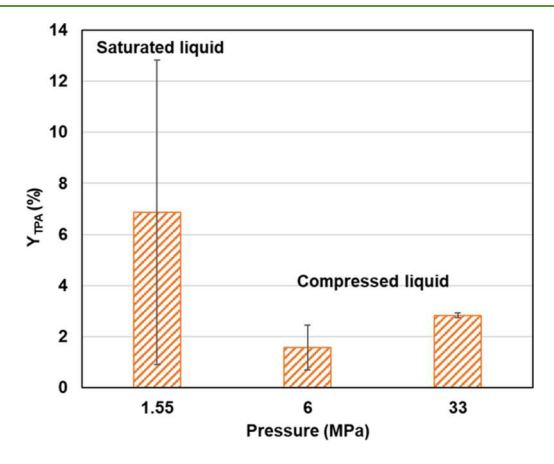


**Figure 1.** TPA yields from hydrolysis (200 °C, 2 h, 1/10 mass ratio PET/water) of PET chips from a sparkling water bottle.

independent of whether water was a saturated (1.55 MPa) or compressed liquid (6 and 33 MPa). Increasing the pressure above saturation provided no apparent benefit. In all three cases, the liquid volume fraction in the reactor was at least 0.95, so hydrolysis was taking place in either a saturated or a compressed liquid phase. Figure S6 shows how the dielectric constant, ion product, and density of water change with pressure at T = 200 °C. The changes are modest when water is in the liquid phase, which is consistent with the TPA yields having no statistically significant differences (see Figure 1).

Reactions of PET in solid form with saturated vapor showed that the TPA yield increased by 8 wt % upon decreasing the fraction of the reactor volume occupied by liquid water from 0.95 to 0.19 (see Figure S8). While this suggests that increasing the fraction of the reactor volume occupied by saturated vapor improves PET hydrolysis, future work is required to confirm and interrogate this observation.

*PET Hydrolysis at Constant Pressure.* Figure 2 shows the TPA yield from hydrolysis in superheated vapor (T=350 and 400 °C), saturated liquid (T=311 °C), and compressed liquid water (T=200 and 260 °C) for t=30 min at 10 MPa. All runs save that at T=200 °C were done above  $T_{\rm m,PET}$ , so the plastic

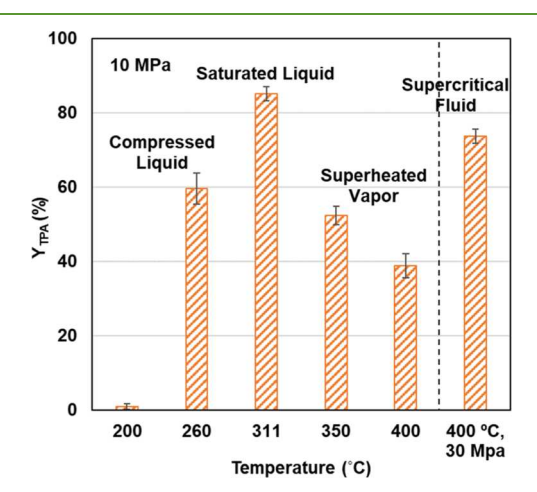


**Figure 2.** TPA yields from hydrolysis (10 MPa or 30 MPa, 30 min, 1/10 mass ratio PET/water) of PET chips from a sparkling water bottle.

should be in a molten state for hydrolysis under those conditions. The different states of water were achieved by loading different amounts of water into the reactor.

While hydrolysis in compressed liquid water at  $T=200\,^{\circ}\mathrm{C}$  yielded only  $Y_{\mathrm{TPA}}(200\,^{\circ}\mathrm{C},\ 30\,^{\circ}\mathrm{min})=2\%$ , a temperature increase above the melting point of PET (approx.  $T_{\mathrm{m}}=250\,^{\circ}\mathrm{C}$ , see Table 1) was able to improve  $Y_{\mathrm{TPA}}(260\,^{\circ}\mathrm{C},\ 30\,^{\circ}\mathrm{min})=60\%$ . This is due to the influence of temperature on the rate constant and PET's molten state that improves mixing between water and the macromolecules. Additionally, the ion product of water is higher at  $T=260\,^{\circ}\mathrm{C}$  (see Figure S7) and provides a more acidic reaction medium, while its dielectric constant is lower to improve the solubility of hydrocarbon molecules in the reaction medium.

Hydrolysis in saturated liquid water provided the highest  $Y_{TPA}$  (311 °C, 30 min, 10 MPa) = 85% compared to experiments at T = 350 °C and T = 400 °C (both in the superheated vapor phase). Below T = 311 °C, where water is in a liquid state, the ion product remains high, and both density and dielectric constant decrease with increasing temperature (see Figure S7). All three properties show a discontinuous decrease at the liquid/vapor phase transition. Hydrolysis in this gas-like environment gave lower TPA yields even though the temperature was higher and above  $T_{\mathrm{m,PET}}$ . The reduced TPA yields at higher temperatures are likely due to the overreaction of the primary products (e.g., hydrothermal decarboxylation of TPA, char formation). 15 Indeed, the yield of undissolved solids from hydrolysis at T = 311 °C was 1.6 wt %, while hydrolysis at T = 350 and 400 °C yielded 17 wt % undissolved solids. These solids were found to be black powders, suggesting the formation of char during the reaction rather than oligomers from the incomplete conversion of the PET feedstock. The gas yields were 2.4, 12.6, and 14.3 wt % for hydrolysis at T = 311, 350, and 400 °C, respectively. The higher temperatures led to over-reaction and increased yields of solid and gaseous products. Products from hydrolysis at T = 400 °C showed a broad peak at 9 to 12 min in the HPLC chromatogram (Figure S13a), which coincided with the possible TPA decomposition product benzoic acid. 15 Formation of benzoic acid under this condition is consistent with TPA undergoing hydrothermal decarboxylation at T = 350 °C (10–15% conversion) but being stable at T = 300 °C after 1 h. 15

An additional experiment at  $T=400\,^{\circ}\mathrm{C}$  and 30 MPa with the same PET/water mass ratio (1/10) determined the influence of the water density on hydrolysis under supercritical conditions. As shown in Figure 2, the TPA yield increased from 39% at 10 MPa ( $\rho_{\mathrm{water}}=0.038\,\mathrm{g/cm^3}$ ) to 74% at 30 MPa, where the water density was significantly higher ( $\rho_{\mathrm{water}}=0.38\,\mathrm{g/cm^3}$ ). This increased yield is consistent with the more liquid-like reaction environment and higher ion product at 30 MPa, supporting the formation of more hydronium ions to catalyze the reaction (Figure S7). However,  $Y_{\mathrm{TPA}}$  (400 °C, 30 MPa, 30 min) = 74% in denser supercritical water was still lower than that from the milder reaction conditions in saturated liquid,  $Y_{\mathrm{TPA}}$  (311 °C, 10 MPa, 30 min) = 85%. This difference is likely related to more pronounced TPA decomposition at the higher temperature. <sup>15</sup>

A set of experiments were conducted at similar reaction temperatures (within a few degrees of 310  $^{\circ}$ C) but with different water loadings to provide different water phases at the same temperature and decouple the effect of the fluid phase from the effect of temperature. Figure S9 shows that the TPA yields ( $\sim$ 80%) were independent of whether the water phase

was compressed liquid, saturated liquid, saturated vapor, or superheated vapor. These values agree with the TPA yield from hydrolysis in saturated liquid at  $T=311\,^{\circ}\text{C}$  (Figure 2) and support results that show that the vapor phase can be an effective medium for PET hydrolysis (see Figure 1).

Reactions were modeled by a pseudo-first-order reaction to compare the kinetics of PET hydrolysis in the different water phases. The measured amount of the undissolved solids was assumed to be unreacted PET (Table S3) except for runs in superheated vapor at 350 and 400 °C, where the undissolved solids were black, consistent with char formation, as explained above. Figure S10 displays the obtained Arrhenius plot from the kinetic evaluation. The activation energies were  $123 \pm 10$ , 114  $\pm$  11, and 110  $\pm$  13 kJ/mol for PET hydrolysis in compressed liquid, saturated vapor, and saturated liquid water, respectively. The differences in these values are not statistically significant, which indicates that the apparent activation energy is independent of the specific water phase present during hydrolysis. Moreover, these activation energies are consistent with literature values<sup>26</sup> (90–123 kJ/mol) for neutral hydrolysis of PET.

Hydrolysis of Solid or Molten PET in Saturated Liquid Water. As studies indicated that the TPA yield was higher when hydrolysis proceeds in saturated liquid water (see above), a systematic study was undertaken to examine the influence of different temperatures and times on hydrolysis of PET chips immersed in saturated liquid water. Figure 3 shows

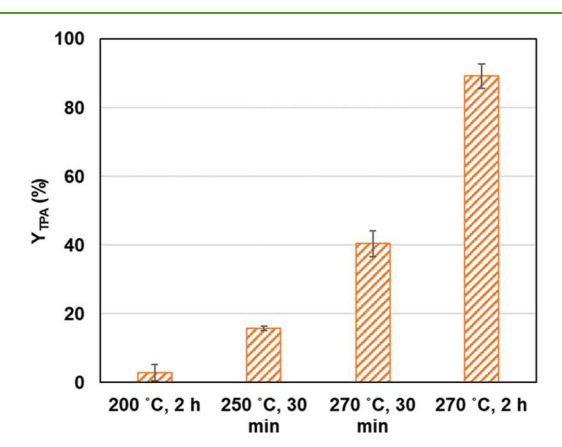


**Figure 3.** Influence of reaction conditions on TPA yields from hydrolysis of chips from sparkling water bottles in saturated liquid water (1/10 PET/water mass ratio; 0.95 liquid volume fraction in the reactor).

TPA yields for the hydrolysis of chips from a PET sparkling water bottle in saturated liquid water at three different temperatures and two different batch holding times (30 min, 2 h). The two runs below the PET melting point gave the lowest TPA yields. A 30 min holding time at  $T=270~^{\circ}\mathrm{C}$  (above  $T_{\mathrm{m,PET}}$ ) gave a yield of about 40%. Increasing the holding time to 2 h improved the yield to 89% (94% on a dry, ash-free basis), which approaches that of complete hydrolysis of the starting material.

Attempts were undertaken to increase the TPA yield at temperatures below the PET melting point (T = 200 °C, t = 2 h) by decreasing the size of the PET particles. The PET sample particle size was reduced to approximately 0.8 mm in diameter (compared to the original chips of  $\sim$ 7 mm). Notably, TPA yields from hydrolysis of particles or chips from an entire bottle were independent of particle size (Figure S11),

suggesting minimal (if any) mass transfer limitations for the described PET hydrolysis approach. The section above on characterization of post-consumer PET also indicated a difference in crystallinity within the different regions of the bottles. Hydrolysis of particles from the bottoms of the sparkling water bottles (38% crystallinity) gave a higher yield  $(Y_{TPA} = 14\%)$  than those obtained from the body (27% initial crystallinity;  $Y_{TPA} = 9\%$ ). This is likely due to reduced solvent penetration into polymer materials with increased crystallinity.<sup>27</sup> In realistic recycling scenarios, such effects can be neglected for mixed particles due to the similar TPA yields for hydrolysis of both chips and particles (~6%, see Figure S11). There were also no notable differences in TPA yields from the different post-consumer PET sources for hydrolysis below  $T_{\rm m,PET}$ . Differences were only visible above  $T_{\rm m,PET}$ , with chips from ketchup bottles having almost 20% more TPA yield than chips from sparkling water bottles at 270 °C (see Figure S12). This suggests that the PET hydrolysis rate depends on the source—likely due to differences in additives, colorants, and the overall manufacturing conditions, which influence thickness and crystallinity.

**Fast Hydrolysis.** Fast hydrolysis experiments were performed to investigate pathways to improve PET depolymerization while limiting byproduct formation. Experiments were conducted by placing a reactor in a sand bath at an elevated temperature (e.g.,  $T_{\rm set\ point}=500\,^{\circ}{\rm C}$ ) and withdrawing it after a short time (i.e.,  $t=1\,$  min). Figure S3 shows that the reactor temperature remains below the sand bath temperature throughout the reaction, and the contents experience rapid heating throughout the short reaction time ( $\sim 5-10\,^{\circ}{\rm C/s}$ ). During fast hydrolysis at  $T_{\rm set\ point}=400,450,500$ , and 550 °C, PET is above its melting temperature for t=12,29,35, and 40 s, respectively (see Figure S3). The Morse potential well approximates the reactor temperature profile within the region of interest. For example, for a set point of 500 °C, the reactor temperature (T in °C and time in seconds) is

$$T = 512(1 - e^{-0.028(t+15)})^2 + 15 (4)$$

The TPA yield from fast hydrolysis (t=1 min) increased as the set point temperature increased from  $T_{\rm set\ point}=400$  to 500 °C (see Figure 4) and reached  $Y_{\rm TPA}$  (500 °C) = 78% (the internal reactor temperature reached 377 °C before being quenched). However, at elevated set point temperatures of

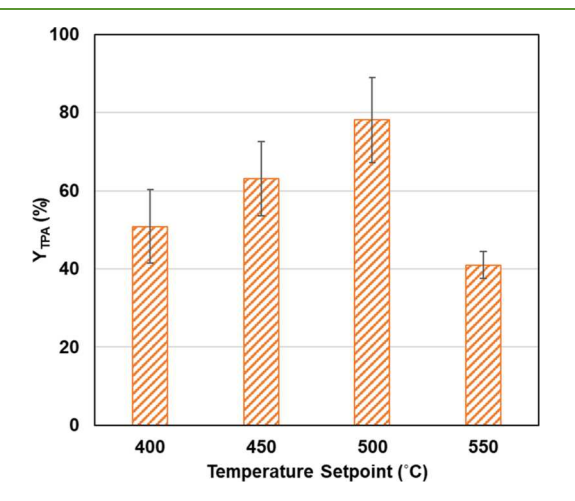
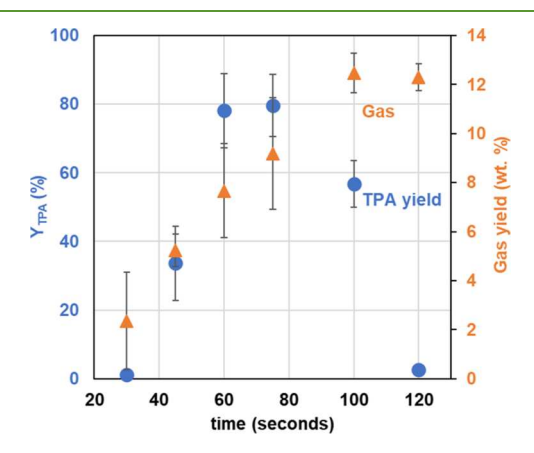


Figure 4. TPA yield from fast hydrolysis of chips from a sparkling water bottle (1 min, 1/10 mass ratio PET/water).

 $T_{\rm set\ point}$  = 550 °C, the TPA yield decreased to 41% (the reactor interior reached T = 418 °C at the one-minute holding mark). This suggests increased TPA decomposition at temperatures exceeding the  $T_{\rm set\ point}$  = 500 °C set point. No TPA was formed at a  $T_{\rm set\ point}$  = 300 °C set point (not shown in Figure 4). While pure TPA gives a single peak at  $\delta$  = 8 ppm for the four aromatic protons in  $^{1}$ H NMR (Figure S15), the suspended solids from the fast hydrolysis experiments ( $T_{\rm set\ point}$  = 400, 500, and 550 °C set points) showed several other peaks in the aromatic region, which indicates the presence of aromatic byproducts. HPLC analysis (Figures S13 and S14) revealed the presence of isophthalic acid, benzoic acid, and bis(2-hydroxyethyl)terephthalate as byproducts.

We also interrogated whether different holding times might improve yield. To this end, fast hydrolysis experiments were conducted with holding times of t = 30-120 s ( $T_{\text{set point}} = 500$  °C). Figure 5 shows a bell-shaped trend for the TPA yield. At t



**Figure 5.** Temporal variation of TPA and gas yields from fast hydrolysis of chips from a sparkling water bottle (500 °C set point, 1/10 mass ratio PET/water).

= 30 s, the reactor temperature reached only  $T=290\,^{\circ}\mathrm{C}$ , and the TPA yield was negligible. The highest yield was achieved at  $t=75\,$  s, where the reactor temperature reached  $T=419\,^{\circ}\mathrm{C}$ . After  $t=120\,$  s, only trace amounts of TPA were obtained. At higher reaction times, increased gas formation was observed (from about 2 wt % at 30 s to 12 wt % at 120 s). This indicated that primary products from hydrolysis further decompose into volatile/gaseous compounds. Products from "fast" hydrolysis at a 500 °C set point and 2 min showed other peaks (that were not TPA, i-TPA, or BHET) not observed at  $t=1\,$  min or  $t=30\,$ s (Figure S13b), indicating the presence of other byproducts.

**Green Chemistry Metrics.** The environmental energy impact,  $\xi$ , was introduced as a metric to assess the potential environmental impacts of PET depolymerization under different process conditions  $^{14,28}$ 

$$\xi = \frac{0.1 \ (m_{\text{water}}/m_{\text{TPA}}) \int_0^t T(t) \ dt}{Y_{\text{TPA}}}$$
 (5)

Here, T is temperature in  ${}^{\circ}C$ , t is time in minutes, and  $m_{\rm water}$  is the mass of water added to the reactor. In prior reports, 10% of the reaction medium  $(m_{\rm water})$  was required as fresh feed, with the remaining 90% being recovered and recycled. This 90% recovery was previously established as typical solvent recycling in industrial processes.  $^{14,29}$   $\xi$  considers the reaction severity and mass of waste generated during the reaction to

Table 3. Environmental Energy Impact (eq 5) for PET Hydrolysis to TPA under Different Reaction Conditions with 1/10 PET/Water Mass Ratio

reference	this study		Mancini and Zanin <sup>8</sup>	Căta et al. <sup>10</sup>		
t (min)	1	30	120	360	120	60
T (°C)	500	311	200	205	300	385
<b>ξ</b> (°C·min)	443	$1.5\times10^4$	$1.3 \times 10^6$	$7.4\times10^4$	$5.0 \times 10^4$	$3.7 \times 10^4$

produce a specific mass of TPA. A more environmentally friendly process has a higher TPA yield, less solvent use, and lower reaction severity, resulting in lower  $\xi$  values. Notably, additional metrics and more robust methods (e.g., life cycle assessment) could be used to assess different PET hydrolysis conditions and approaches.

Table 3 shows the environmental energy impact metric for selected runs with high TPA yields compared to the best (lowest) values from published studies.<sup>8,10</sup>

Hydrolysis in saturated liquid water at  $T=311~^{\circ}\mathrm{C}$  for  $t=30~\mathrm{min}$  led to  $\xi=1.5\times10^4~^{\circ}\mathrm{C}\cdot\mathrm{min}$ , which is in line with results from prior work on isothermal hydrolysis of PET. Reactions at lower temperatures led to larger environmental energy impact values mainly due to the lower TPA yields obtained. For example, experiments at  $T=200~^{\circ}\mathrm{C}$  ( $t=2~\mathrm{h}$ ) had a higher environmental energy impact of  $\xi=1.3\times10^6$ . At  $T>T_{\mathrm{m,PET}}$ , where TPA yields are high (>80%), the reaction time carries more weight. As such, Table 3 shows that experiments at  $T=311~^{\circ}\mathrm{C}$  ( $t=30~\mathrm{min}$ ) have a lower environmental energy impact than those described in literature at  $T=300~(t=120~\mathrm{min})$  or  $T=385~^{\circ}\mathrm{C}$  ( $t=60~\mathrm{min}$ ).

Fast hydrolysis at  $T=500\,^{\circ}\mathrm{C}$  and  $t=1\,\mathrm{min}$  resulted in a much lower environmental energy impact metric (443  $^{\circ}\mathrm{C\cdot min}$ ) than did isothermal hydrolysis at  $T=311\,^{\circ}\mathrm{C}$  and  $t=30\,\mathrm{min}$ . This value was the lowest from the results presented thus far and lower than those given in previous published work on neutral hydrolysis of PET. We wondered whether an even further reduction in the environmental energy impact metric could be realized by increasing the PET/water ratio used in fast hydrolysis. An additional experiment with a PET/water mass ratio of 1:3 (rather than 1:10) yielded  $Y_{\mathrm{TPA}}$  (500  $^{\circ}\mathrm{C}$ , 1 min, 1:3) = 69% and an even lower environmental energy impact of 235  $^{\circ}\mathrm{C\cdot min}$ .

# CONCLUSIONS

Fast hydrolysis was shown to be a promising new approach for the chemical recycling of post-consumer PET. High yields (>80%) and short reaction times (e.g., 60 s) led to the lowest (best) environmental energy metrics reported to date for uncatalyzed PET hydrolysis. This fast hydrolysis approach requires further optimization to lead to higher yields of TPA with lower capital cost and environmental impact at scale.

PET hydrolysis proceeds in compressed liquid, saturated vapor, superheated vapor, and supercritical water phases under the conditions examined, but the present work revealed no advantage to using these conditions for isothermal hydrolysis in lieu of saturated liquid water. A potential drawback of supercritical conditions is that the higher temperatures promote the decomposition of the monomers via secondary reactions. While isothermal hydrolysis in saturated liquid water was effective, it carried a larger environmental energy impact metric compared to fast hydrolysis. Isothermal hydrolysis of PET in its solid state (below the melting point) proceeded more slowly but gave a modestly higher TPA yield when conducted in saturated vapor compared with saturated liquid.

Even so, the TPA yields from neutral hydrolysis of solid PET were consistently below 20% under the conditions examined.

PET hydrolysis above the PET melting point seems to depend on the PET source, being affected by particle size, crystallinity, and colorant content. Additional work is needed to elucidate the effects of the variability in post-consumer PET sources (e.g., crystallinity, thickness, additives, and colorants) on the hydrolysis rates and then capture those effects in reaction models. This additional experimental and modeling work would facilitate the design and techno-economic assessment of conceptual PET hydrolysis processes at scale.

## ASSOCIATED CONTENT

# Supporting Information

The Supporting Information is available free of charge at https://pubs.acs.org/doi/10.1021/acssuschemeng.3c00946.

Average dimensions of plastic chips and characterization results; temperature profiles of reactor contents and temperatures; water property changes with temperature and pressure, TPA yields; reactor setup for reactions under vapor and TPA yields for such reactions; TPA yields for hydrolysis at 308–312 °C at 10 and 30 min; Arrhenius plot for the PET neutral hydrolysis; yields of undissolved solids and TPA from chips and particles from different portions of the bottles; TPA yields using different PET bottles; HPLC chromatograms and LC–MS selective ion chromatograms of the aqueous phase from PET hydrolysis; and <sup>1</sup>H NMR spectra and MALDI-TOF MS analysis of oligomers for different PET hydrolysis experiments (PDF)

## AUTHOR INFORMATION

# **Corresponding Authors**

Phillip E. Savage — Department of Chemical Engineering, The Pennsylvania State University, State College, Pennsylvania 16802, United States; orcid.org/0000-0002-7902-3744; Email: psavage@psu.edu

Christian W. Pester — Department of Chemical Engineering, The Pennsylvania State University, State College, Pennsylvania 16802, United States; Department of Chemistry and Department of Materials Science and Engineering, The Pennsylvania State University, State College, Pennsylvania 16802, United States; Orcid.org/0000-0001-7624-4165; Email: cup280@psu.edu

#### Author

Patrícia Pereira — Department of Chemical Engineering, The Pennsylvania State University, State College, Pennsylvania 16802, United States

Complete contact information is available at: https://pubs.acs.org/10.1021/acssuschemeng.3c00946

#### Note:

The authors declare no competing financial interest.

#### ACKNOWLEDGMENTS

This material is based upon work supported by the National Science Foundation under Grant EFRI E3P number 2029397. The authors thank Dr. Yanyu Mu and Prof. Robert Rioux for helpful discussions on HPLC use and LC-MS. The authors thank Liza Wilson from the Penn State DOE Center for Lignocellulose Structure and Formation for the use of the Wiley Mill. The authors acknowledge the Penn State Materials Characterization Lab for the use of thermogravimetric differential scanning calorimetry and x-ray spectroscopy. Dr. Ekaterina Bazilevskaya, Dr. Bob Hengstebeck, and Gino Tamborine collected the TG-DSC data, XPS data, and DSC data, respectively. The authors are also thankful to the Proteomics and Mass Spectrometry Core Facility at the Huck Institute of Life Sciences, especially to Dr. Tatiana Laremore for assisting in preparing samples and interpreting MALDI-TOF MS data.

## REFERENCES

- (1) FAQs on Plastics—Our World in Data. https://ourworldindata.org/faq-on-plastics (accessed Jan 28, 2021).
- (2) Plastics: Material-Specific Data, Facts and Figures about Materials, Waste and Recycling; US EPA. https://www.epa.gov/facts-and-figures-about-materials-waste-and-recycling/plastics-material-specific-data (accessed Feb 1, 2021).
- (3) Welle, F. Twenty Years of PET Bottle to Bottle Recycling—An Overview. *Resour., Conserv. Recycl.* **2011**, *55*, 865–875.
- (4) Kumartasli, S.; Avinc, O. Important Step in Sustainability: Polyethylene Terephthalate Recycling and the Recent Developments; Muthu, S. S., Gardetti, M. A., Eds.; Sustainability in the Textile and Apparel Industries, Sustainable Textiles: Production, Processing, Manufacturing & Chemistry; Springer Nature Switzerland, 2020; pp 1–20. DOI: DOI: 10.1007/978-3-030-38013-7 1.
- (5) Jankauskaitè, V.; Macijauskas, G.; Lygaitis, R. Polyethylene Terephthalate Waste Recycling and Application Possibilities: A Review. *Polym. Compos.* **2008**, *14*, 119–127.
- (6) Scheirs, J.; Long, T. E. Modern Polyesters: Chemistry and Technology of Polyesters and Copolyesters; John Wiley & Sons, Ltd, 2003
- (7) Zhang, S.; Xu, W.; Du, R.; Zhou, X.; Liu, X.; Xu, S.; Wang, Y. Z. Cosolvent-Promoted Selective Non-Aqueous Hydrolysis of PET Wastes and Facile Product Separation. *Green Chem.* **2022**, 24, 3284–3292.
- (8) Mancini, S. D.; Zanin, M. Optimization of Neutral Hydrolysis Reaction of Post-Consumer PET for Chemical Recycling. *Prog. Rubber, Plast. Recycl. Technol.* **2004**, 20, 117–132.
- (9) Valh, J. V.; Vončina, B.; Lobnik, A.; Zemljič, L. F.; Škodič, L.; Vajnhandl, S. Conversion of Polyethylene Terephthalate to High-Quality Terephthalic Acid by Hydrothermal Hydrolysis: The Study of Process Parameters. *Text. Res. J.* **2020**, *90*, 1446–1461.
- (10) Căta, A.; Miclău, M.; Ienaşcu, I.; Ursu, D.; Tănasie, C.; Ştefănuţa, M. N. Chemical Recycling of Polyethylene Terephthalate (PET) Waste Using Sub- and Supercritical Water. *Rev. Roum. Chim.* **2015**, *60*, 579–585.
- (11) Güçlü, G.; Yalçinyuva, T.; Özgümüş, S.; Orbay, M. Simultaneous Glycolysis and Hydrolysis of Polyethylene Terephthalate and Characterization of Products by Differential Scanning Calorimetry. *Polymer* **2003**, *44*, 7609–7616.
- (12) Campanelli, J. R.; Cooper, D. G.; Kamal, M. R. Catalyzed Hydrolysis of Polyethylene Terephthalate Melts. *J. Appl. Polym. Sci.* **1994**, *53*, 985–991.
- (13) Colnik, M.; Knez, Z.; Škerget, M. Sub-and Supercritical Water for Chemical Recycling of Polyethylene Terephthalate Waste. *Chem. Eng. Sci.* **2021**, 233, 116389.
- (14) Barnard, E.; Rubio Arias, J. J.; Thielemans, W. Chemolytic Depolymerisation of PET: A Review. *Green Chem.* **2021**, 23, 3765–3789.

- (15) Dunn, J. B.; Burns, M. L.; Hunter, S. E.; Savage, P. E. Hydrothermal Stability of Aromatic Carboxylic Acids. *J. Supercrit. Fluids* **2003**, *27*, 263–274.
- (16) Zhang, Y.-M.; Sun, Y.-Q.; Wang, Z.-J.; Zhang, J. Degradation of Terephthalic Acid by a Newly Isolated Strain of Arthrobacter Sp.0574. S. Afr. J. Sci. 2013, 109, 4.
- (17) Karayannidis, G. P.; Chatziavgoustis, A. P.; Achilias, D. S. Poly(ethylene terephthalate) recycling and recovery of pure terephthalic acid by alkaline hydrolysis. *Adv. Polym. Technol.* **2002**, 21, 250–259.
- (18) Al-Sabagh, A. M.; Yehia, F. Z.; Eshaq, G.; Rabie, A. M.; ElMetwally, A. E. Greener Routes for Recycling of Polyethylene Terephthalate. *Egypt. J. Pet.* **2016**, 25, 53–64.
- (19) Yoshioka, T.; Okayama, N.; Okuwaki, A. Kinetics of Hydrolysis of PET Powder in Nitric Acid by a Modified Shrinking-Core Model. *Ind. Eng. Chem. Res.* **1998**, *37*, 336–340.
- (20) Ravens, D. A. S.; Ward, I. M. Chemical Reactivity of Polyethylene Terephthalate. Hydrolysis and Esterification Reactions in the Solid Phase. *Trans. Faraday Soc.* **1961**, *57*, 150–159.
- (21) Zope, V. S.; Mishra, S. Kinetics of Neutral Hydrolytic Depolymerization of PET (Polyethylene Terephthalate) Waste at Higher Temperature and Autogenious Pressures. *J. Appl. Polym. Sci.* **2008**, *110*, 2179–2183.
- (22) Motavaf, B.; Savage, P. E. Effect of Process Variables on Food Waste Valorization via Hydrothermal Liquefaction. *ACS ES&T Engg* **2021**, *1*, 363–374.
- (23) Scott, D. S.; Czernik, S. R.; Piskorz, J.; Radlein, D. S. A. G. Fast Pyrolysis of Plastic Wastes. *Energy Fuels* **1990**, *4*, 407–411.
- (24) Sichina, W. J. DSC as Problem Solving Tool: Measurement of Percent Crystallinity of Thermoplastics, 2000.
- (25) Akiya, N.; Savage, P. E. Roles of Water for Chemical Reactions in High-Temperature Water. *Chem. Rev.* **2002**, *102*, 2725–2750.
- (26) Zhang, L. Kinetics of Hydrolysis of Poly(Ethylene Terephthalate) Wastes Catalyzed by Dual Functional Phase Transfer Catalyst: A Mechanism of Chain-End Scission. *Eur. Polym. J.* **2014**, 60, 1–5.
- (27) Ügdüler, S.; Van Geem, K. M.; Denolf, R.; Roosen, M.; Mys, N.; Ragaert, K.; De Meester, S. Towards Closed-Loop Recycling of Multilayer and Coloured PET Plastic Waste by Alkaline Hydrolysis. *Green Chem.* **2020**, 22, 5376–5394.
- (28) Sheldon, R. A. The E Factor 25 Years on: The Rise of Green Chemistry and Sustainability. *Green Chem.* **2017**, *19*, 18–43.
- (29) Rubio Arias, J. J.; Thielemans, W. Instantaneous Hydrolysis of PET Bottles: An Efficient Pathway for the Chemical Recycling of Condensation Polymers. *Green Chem.* **2021**, 23, 9945–9956.